

Comparison between Experimental, Nonlinear Finite Element Analysis Results and International Codes for Reinforced Concrete Flat Slabs Strengthened Using Different Techniques to Resist Punching Failure

Hanna F. H. Habeb¹, Ahmed A. Mahmoud*², Alaa G. Sherif³, Magdy M.M. Genidi⁴

¹*Corresponding author, Tel: 20201005679172, E-mail: ahmed.ahmed@feng.bu.edu.eg, ahmed.m5882@gmail.com
Department of Civil Engineering, Faculty of Engineering at Shoubra, Benha University-, 108 Shoubra Street, Shoubra 11691, Cairo, Egypt.

²Higher Institute of Engineering, 15th of May City, Egypt (E-mail: civil.hanafakhry@yahoo.com).

³Professor, Faculty of Engineering (Shoubra), Benha University, Egypt (E-mail: ahmed.ahmed@feng.bu.edu.eg and ahmed.m5882@gmail.com);

⁴Professor of Reinforced Concrete Structures, Civil Engineering Dept., (Structure), Faculty of Engineering El Matarya- Helwan University, Cairo, Egypt (E-mail: alaa_sherif@m-eng.helwan.edu.eg and agbsherif@gmail.com);

⁵Associate Professor, Civil Engineering Dept., (Structure), Faculty of Engineering El Matarya- Helwan University, Cairo, Egypt (E-mail: magdy_genedy@m-eng.helwan.edu.eg and magdy_genidi@yahoo.com).

Abstract: The main objectives of this research are to study experimentally, analytically and numerically the effectiveness of the proposed external strengthening techniques to resist punching shear of reinforced concrete flat slabs. The finite element (FE) analysis software program (ANSYS V. 19) was used to create the models and investigate the effects of some parameters on punching shear of reinforced concrete flat slabs. Eight variable parameters are taken into consideration during study full scale flat slab models to account the influence of: (1) concrete compressive strength f_{cu} ; (2) reinforcing steel yield strength f_y ; (3) slab thickness (t_s); (4) shear studs and stirrups diameter (D_b); (5) shear studs (stirrups) spacing / t_s ratio (S_b/t_s); (6) shear studs stirrups spacing/ t_s ratio (D/t_s); (7) main steel ratio/ m_{max} (m/m_{max}); (8) top steel ratio/ m_{max} (m'/m_{max}). The numerical results were compared with the analytical results calculated from ECP 203-2017 [1] and ACI 318-19 [2]. The comparison showed a great match between the numerical results and the results of the two codes, especially ACI 318-19 [2].

Keywords: Punching shear, experimental, external strengthening, ANSYS program, numerical analysis.

I. INTRODUCTION

A flat slab floor system is often the choice when there is a need for more clear head such as car parks, libraries and multi-story buildings where larger spans are also required.

Punching shear failure is a major problem encountered in the design of reinforced concrete flat slabs. Many researchers have studied the punching shear behavior of reinforced concrete flat slabs [3]. The punching shear strength and deformation capacity are strongly influenced by the type and characteristics of the shear reinforcing system [4]. The slabs punching shear reinforcing system are: (1) separated stirrups, (2) continuous stirrups, (3) bonded reinforcement with

anchorage plates, (4) steel plates, (5) continuous FRP sheets, (6) FRP strips, (7) internal prestressing, (8) external prestressing, (9) bent up bars, (10) vertical studs, and (11) inclined studs.

Failures of flat slab structures were reported during construction and brittle failure happens with no enough warnings. The experimental results showed that the increase of concrete strength leads to increase of ultimate load of the slab and flat slabs resisting by steel fiber reinforcement have the highest punching shear resistance comparing to its corresponding slabs resisting by added straight bars [5].

There are many researches that talk about external strengthening to resist punching shear [6]. Because experimental tests take a long time and are expensive, it was essential for the researchers to find less expensive methods, so they turned to use various methods of modeling concrete structures using both numerical and analytical methods [7].

II. NONLINEAR FINITE ELEMENT ANALYSIS

The following steps were taken in order to analyze the considered slabs specimens: (1) selection of element type; (2) assigning material properties; (3) modeling and meshing volume; (4) applying loads and boundary conditions, then solving [8]. Flat slab reinforced concrete was modeled using SOLID65. The reinforcing bars, steel shear studs and GFRP stirrups were idealized using a 2-node bar (linear) named (Link 180) as shown in Fig. 1.

The tested slabs discretized using equal-size 3-D isoperimetric elements (25*25*25 mm) Solid 65 as shown in Fig. 2. The column stub was represented as shown in the figure to simulate the actual shape and dimensions of column stub of the tested specimens. The slabs were analyzed as simply supported along the four sides to simulate the experimental set-up.

Referring to ANSYS V19 technical manual [8], the three-dimensional isoparametric element Solid65 was adopted to model the concrete elements. Solid 65 element is capable of cracking in tension and crushing in compression. This element is similar to the one recommended., which introduced a three-dimensional, 8-node isoparametric element.

Solid 65 element is defined by eight nodal points each having three translational degrees of freedom x, y, and z (and no rotational deformations), along with a 2 x 2 x 2 Gaussian integration scheme which is used for the computation of the element stiffness matrix. The software package "ANSYS V. 19.0" [8] allows steel reinforcement to be defined using the smeared reinforcement approach, in which the amount of reinforcement is defined by specifying a volume ratio and orientation angles of the rebar.

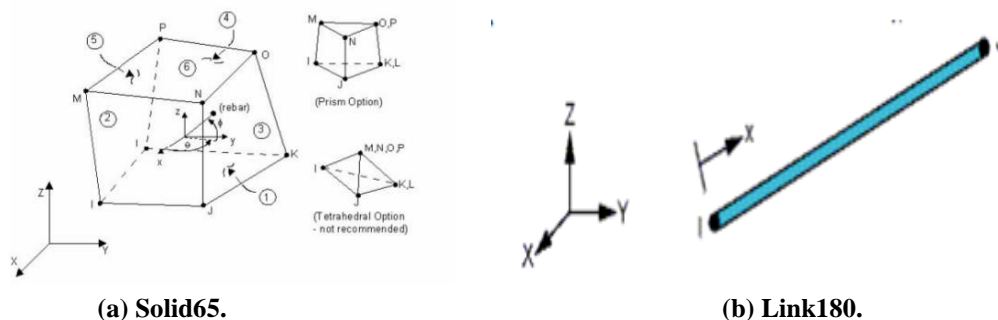


Fig. 1: Elements Geometry [9].

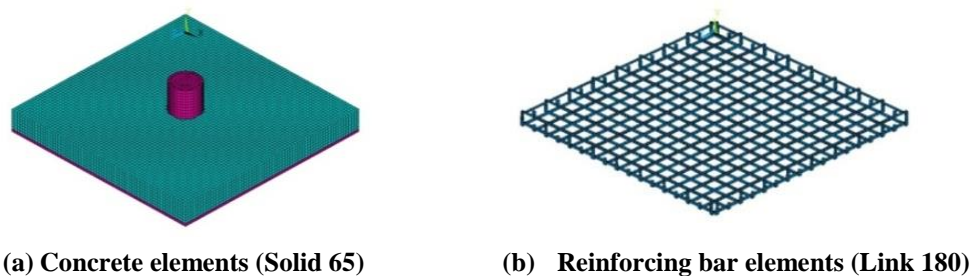


Fig. 2: ANSYS idealization of the slabs.

III. VERIFICATION AND FALIDATION

III.I Details of studied slabs

One slab from Hanna, F.H.H. [9] (named Sc) was used to verify the numerical and the analytical results. The average cubic and cylindrical concrete compressive strength were 26 and 22 MPa, respectively. The cracking strength of concrete was taken as 10% of the concrete compressive strength.

A fiberglass is a custom of fiber-reinforced plastic. Fiberglass is strong, less brittle and lightweight. The best advantage fiberglass is its ability to get shaped in different difficult shapes. The used Epoxy was Sikadur -165 which is also a product of Sika construction company as well.

Shear bolts have diameter 16 mm and length 180 mm with a nut. Shear bolts are installed in holes drilled in the slab shortly before testing. The holes were drilled perpendicular to the slab plane using 16 mm diamond coring bits. The shear bolts were arranged in concentric rows parallel to the perimeter of the column. Figure 3 shows the slab dimensions and reinforcement details. The slab has 1700 mmx1700 m and thickness 150 mm with a circular column has 250 mm diameter. Figure 3 shows the typical dimensions and reinforcement details of slab Sc [9].

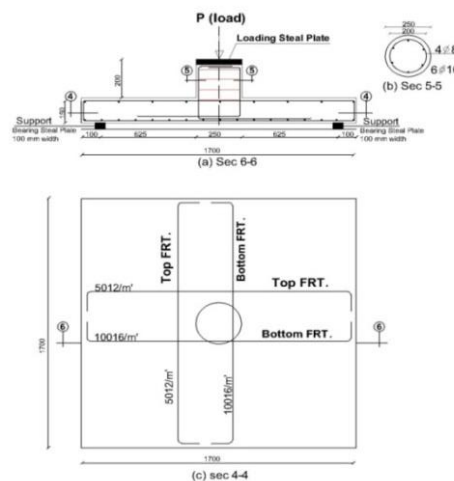


Fig. 3: Typical dimensions and reinforcement details of slab Sc [9].

III.II Comparison between the experimental and numerical results

Figure 4 shows a comparison of the experimental and the predicted load-deflection curves, revealing excellent responses to the numerical model's accuracy at various response stages. The ultimate load, P_u , deflection at ultimate load, Δu and secant stiffness, S.S which defined as the ratio of the ultimate load to the corresponding displacement were estimated. Table 1 shows comparison between the numerical and the experimental results of slab Sc.

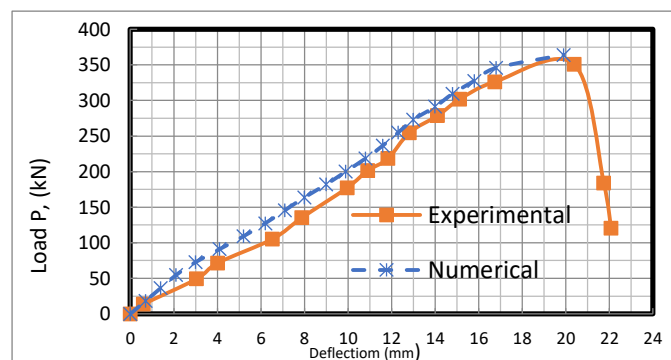


Fig. 4: Experimental and numerical load-deflection curve for slab Sc [9].

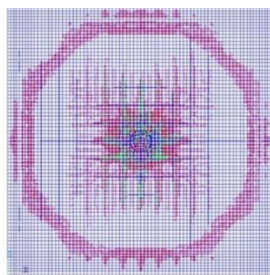
TABLE I: COMPRISON BETWEEN THE NUMERICAL AND THE EXPERRIMENTAL RESULTS OF SLAB Sc [9].

Comparison	Experimental [27]	Numerical [FE]	Exp. [27]/Num. [FE]
Ultimate load, (P_u), kN	351.01	364	0.96
Deflection at ultimate load, (Δ_u) mm	20.386	19.92	1.023
Secant stiffness (S.S), kN/ mm	17.22	18.27	0.94

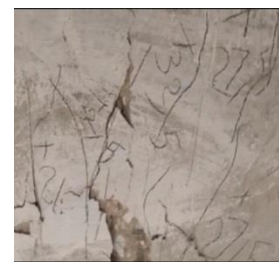
The following conclusions were reached after comparing the numerical and the experimental results as shown in Fig. 4 and Table 1:

1. The finite element predictions have been close to the experimental results at the ultimate level.
2. The ratio [$P_{u\text{exp}}/P_{uFE}$] is 0.96. The ratio [$\Delta_{uEXP} / \Delta_{uFE}$] is 1.023 and the secant stiffness ratio is ($S.S_{(EXP.)} / S.S_{(FE)}$) = 0.95.

Early flexure cracks for Sc appeared at the middle of the slab span and became more spread as the load increased as shown in Fig.5. Figure 5 shows a very good agreement between the experimental and the numerical cracks pattern.



(a) Predicted cracks pattern.



(b) Experimental cracks pattern.

Fig. 5: Cracks pattern of experimental and the predicted model for slab.

IV. PARAMETRIC NUMERICAL STUDY

IV.1 Details of the studied slabs

Figure 6 shows the geometry and reinforcement details of the parametric studied slabs. Ten groups are described in Table 3 and analyzed by ANSYS rogram.19. All slabs 2000 mm x 2000 mm, slab thickness 200 mm, $f_{cu} = 25$ Mpa and $f_y = 350$ Mpa with a column circular diameter 400 mm ($A_s = 8F16$). S1 was the first control slab (reference slab for 24 slabs divided into 8 groups as shown in Table 2) with shear studs (bolts) diameter 8 mm, with spacing ($0.5 t_s$) 100 mm, one row with distance 200 mm (t_s) from column face and main steel ratio/ m_{max} (m / m_{max}) = 0.3 and compression steel ratio/ m_{max} (m' / m_{max}) = 0.2 without drop panel..

TABLE II: DETILES OF THE STUDIED SLABS.

Group	Slab NO	Studied Parameters								Notes
		f_{cu} (MPa)	f_y (MPa)	Slab Thick-ness (mm)	Shear Studs (Stirrups) Diamet-er	Shear Studs (Stirrups) Spacing/ t slab	Shear Studs (Stirrups) Distance s/t slab	μ / μ_{max}	μ' / μ_{max}	
Control Specimen	S1	25	350	20	8	0.5	1	0.4	0.2	Control Specimen
Group (1) C	S2	30	350	20	8	0.5	1	0.4	0.2	Effect of f_{cu}
	S3	35	350	20	8	0.5	1	0.4	0.2	
	S4	40	350	20	8	0.5	1	0.4	0.2	
Group (2) C	S5	25	240	20	8	0.5	1	0.4	0.2	Effect of f_y
	S6	25	400	20	8	0.5	1	0.4	0.2	
	S7	25	420	20	8	0.5	1	0.4	0.2	
Group (3)	S8	25	350	22	8	0.5	1	0.4	0.2	Effect of

C	S9	25	350	24	8	0.5	1	0.4	0.2	the Slab Thickness
	S10	25	350	26	8	0.5	1	0.4	0.2	
Group (4) C	S11	25	350	20	6	0.5	1	0.4	0.2	Effect of Shear Studs Diameter
	S12	25	350	20	10	0.5	1	0.4	0.2	
	S13	25	350	20	12	0.5	1	0.4	0.2	
Group (5) C	S14	25	350	20	8	0.75	1	0.4	0.2	Effect of Shear Studs Spacing / t _{slab}
	S15	25	350	20	8	1	1	0.4	0.2	
	S16	25	350	20	8	1.25	1	0.4	0.2	
Group (6) C	S17	25	350	20	8	0.5	0.5	0.4	0.2	Effect of Shear Studs Distances/t _{slab}
	S18	25	350	20	8	0.5	1.5	0.4	0.2	
	S19	25	350	20	8	0.5	2	0.4	0.2	
Group (7) C	S20	25	350	20	8	0.5	1	0.3	0.2	Effect of Main Steel Ratio/ μ_{max}
	S21	25	350	20	8	0.5	1	0.5	0.2	
	S22	25	350	20	8	0.5	1	0.6	0.2	
Group (8) C	S23	25	350	20	8	0.5	1	0.4	0.15	Effect of Top Steel Ratio/ μ_{max}
	S24	25	350	20	8	0.5	1	0.4	0.25	
	S25	25	350	20	8	0.5	1	0.4	0.3	

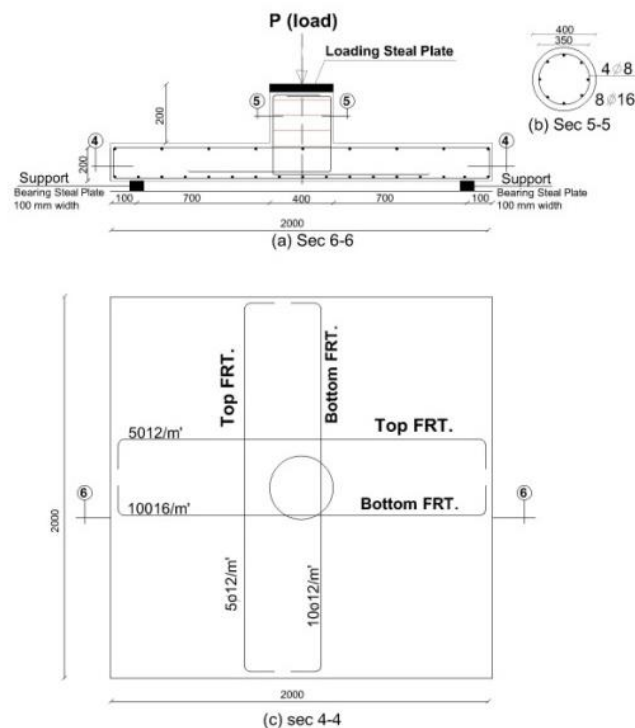


Fig.6: Geometry and reinforcement details of the parametric studied slabs.

IV.II Analysis of the numerical results

The load-deflection curves showed the behavior of the slabs by displaying a variety of response parameters, including ultimate load, deflection, and secant stiffness. Figure 7 and Table 3 shows the effect of some parameters affecting the punching shear behavior.

TABLE III: NUMERICAL RESULTS OF THE STUDIED SLABS.

Slab No.	Numerical Ultimate Load, (P_u) (kN)	Deflection at Ultimate Load (Δ_u) (mm)	Secant Stiffness (S.S) (kN/mm)	$P_u/P_{u S1}$ %	$\Delta_u/\Delta_{u S1}$ %	S.S/S.S _{S1} %
S1	1056	74.84	14.11	100	100	100
S2	1188	69.12	17.19	112.5	92.36	121.83
S3	1276	66.09	19.31	120.83	88.30	136.85
S4	1364	63.39	21.52	129.17	84.70	152.51
S5	968	80.12	12.08	91.68	107.06	85.61
S6	1144	65.05	17.59	108.33	86.92	124.66
S7	1188	60.84	19.53	112.50	81.29	138.41
S8	1188	70.12	16.94	112.5	93.69	120.05
S9	1320	66.13	19.96	125	88.36	141.45
S10	1452	63.84	22.74	137.5	85.30	161.16
S11	968	77.85	12.43	91.66	104.02	88.09
S12	1144	70.61	16.20	108.33	94.34	114.81
S13	1232	64.91	18.98	116.66	86.73	134.51
S14	968	77.17	12.54	91.66	103.11	93.85
S15	880	78.93	11.15	83.33	105.46	79.02
S16	792	80.63	9.82	75	107.73	69.59
S17	792	70.10	11.30	75	93.66	80.08
S18	1188	70.61	16.82	112.5	94.34	110.20
S19	1364	71.59	19.05	129.16	95.65	135.01
S20	968	83.63	11.57	91.66	111.74	81.99
S21	1144	64.03	17.87	108.33	85.55	126.62
S22	1232	55.09	22.38	116.66	73.61	158.61
S23	924	83.56	11.06	87.50	111.65	78.37
S24	1100	65.96	16.67	104.16	88.13	118.19
S25	1188	57.17	20.78	112.50	76.39	147.27

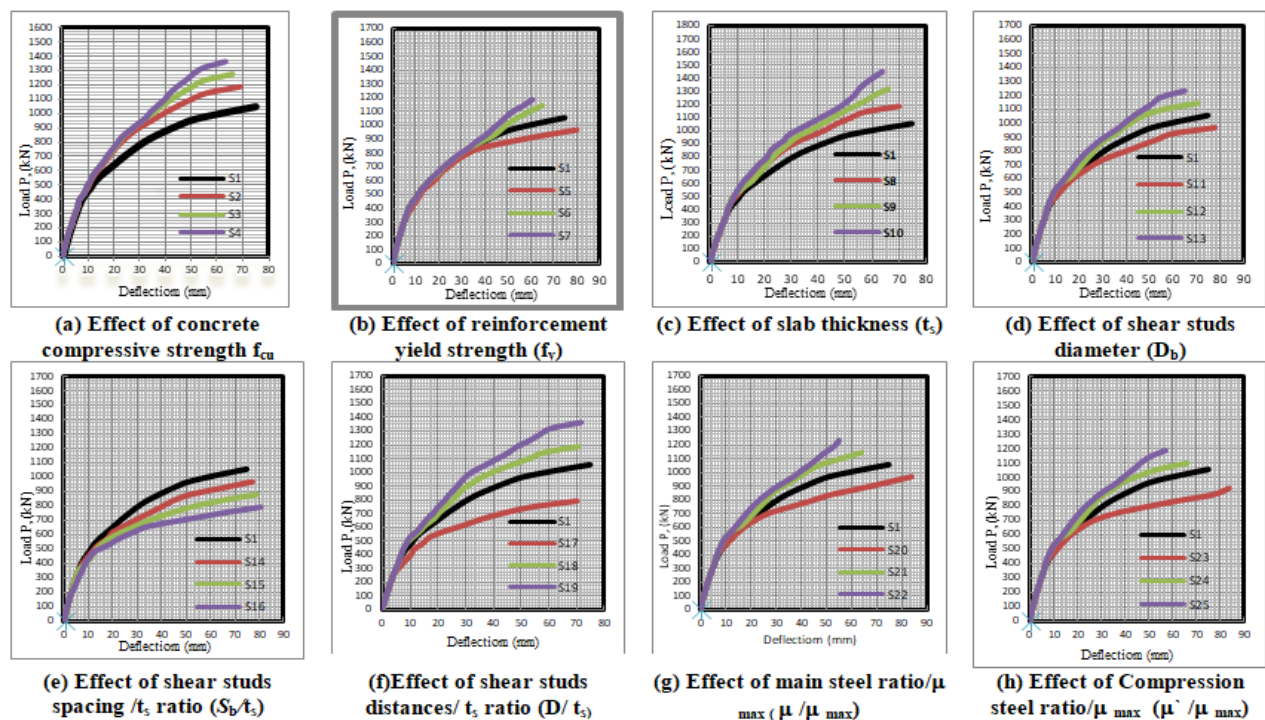


Fig. 7: Load -deflection curves of all parametric studied slabs.

IV.III Effect of concrete compressive strength (f_{cu})

The concrete strength increased, higher ultimate loads reached with a noticeable small decrease in deformation at the same load levels. Four slabs have the concrete compressive strength (f_{cu}) 25, 30, 35 and 40 MPa for slabs S1, S2, S3 and S4 respectively. Table 4 shows the ultimate load of slabs S2, S3 and S4, is larger than of slab S1 (reference slab) by 12.5%, 20.83% and 29.75%, respectively. In addition to the secant stiffness of slabs S2, S3 and S4, is larger than that of slab S1 by 21.83%, 36.85%, and 52.51%, respectively, although the corresponding deflections are 7.64%, 11.7%, and 15.3 % respectively lower than slab S1(reference slab). It can be noted that, the increase of the concrete compressive strength, the increase in the ultimate load and the secant stiffness, and decrease in the deflection.

IV.IV Effect of reinforcement yield strength (f_y)

As shown in Fig. 7.b, the load deflection curves are approximately the same for all slabs of group 2 at the beginning, while it varied according to the reinforcement yield strength (f_y) near the ultimate load. Based on Table 4, the ultimate load of slab S5 is less than that of slab S1 by 8.32% but slabs S6 and S7 has larger ultimate load than of that of slab S1 by 8.33% and 12.50%, respectively. In addition to the ultimate deflection of slab S5 is larger than of that of slab S1 by 7.06% but S6 and S7 is less than of that slab S1 by 13.08 %, and 18.71% respectively, although the corresponding secant stiffness of slab S5 is less than of slab S1 by 7.63% but S6 and S7 is larger than of slab S1 by 20.69 %, and 31.5%, respectively. It is clear that, the higher the reinforcement yield strength f_y , the small higher the ultimate load, secant stiffness and the lower the deflection.

IV.V Effect of slab thickness (t_s)

Figure 7.c shows the effect of increase slab thickness (t_s) on the ultimate load, secant stiffness and the deflection using three slabs S8, S9 and S10 compared to S1(reference slab). It can be noted that, an increase in both the ultimate load and secant stiffness while a decrease in deflection has been occurred as shown in Table 4.

IV.VI Effect of shear studs (stirrups) diameter (D_b)

From Table 4 the ultimate load and secant stiffness of slab S11 is less than that of slab S1 by (8.34 % and 11.91%) but S12 and S13 is larger than that of slab S1 by (8.33% and 14.81%) and (16.66% and 34.51) respectively. In addition to the ultimate deflection of slab S11 is larger than that of slab S1 by 7.06 % while slabs S12 and S13 has ultimate deflection less than that of slab S1 by 13.08%, and 18.71% respectively. From Fig. 7.d it can be noted that the decrease of (D_b) decrease the ultimate load and secant stiffness and increasing deflection and vice versa.

IV.VII Effect of shear studs (stirrups) spacing / t_s ratio (S_b/t_s)

Four slabs S1, S14, S15 and S16 has (S_b/t_s) 0.5, 0.75, 1 and 1.25 respectively. Increasing shear studs spacing (S_b) has a noticeable effect on the three slabs S14, S15 and S16, where both the ultimate load and secant stiffness decreased with an increase in the deflection as shown in Table 4 and Fig 7.e. The ultimate load and secant stiffness of slabs S14, S15 and S16 are less than that of slab S1 by (8.34% and 6.15%), (16.67% and 20.98%) and (25% and 30.41%) respectively, with an increase in deflection by 3.11%, 5.46% and 7.73% respectively compared to S1 (reference slab).

IV.VIII Effect of shear studs (stirrups) distances/ t_s ratio (D/t_s)

Group 6, study the effect of distance of shear studs (bolts) row from column face (D) where taken ratio (D/t_s) 1.0, 0.50, 1.5 and 2 for slabs S1, S17, S18 and S19 respectively where S1 is the reference slab. Table 4 shows an increase in both the ultimate load and secant stiffness at increase (D) and vice versa while the deflection very decreased when increase or decrease (D). The ultimate load and secant stiffness of slab S17 is less than of slab S1 by (25% and 19.92%) but S18 and S19 is larger than of that of slab S1 by (12.5% and 10.20%) and (29.16% and 35.01) respectively. In addition to the ultimate deflection of slab S17, S18 and S19 is very small less than that of slab S1 by 6.34%, 5.66% and 4.35% respectively.

IV.IX Effect of main steel ratio/ μ_{max} (μ/μ_{max})

Table 4 and Fig 7.g showed that increasing the main steel ratio/ μ_{max} increasing the ultimate load decrease the deflection leads to large secant stiffness while, the ultimate load and secant stiffness decreased and large deflection due to decreasing main steel ratio/ μ_{max} . Increased and decreasing proportions ultimate load and secant stiffness, reduction and increasing ratios deflection for three slabs S20, S21 and S22 compared to S1 control specimen showed in Table 4. The ultimate deflection of slab S20 is larger than of slab S1 by 11.74% but S21 and S22 has ultimate deflection less than of that of slab S1 by 14.45%, and 26.39% respectively.

IV.X Effect of compression steel ratio/ m_{max} (m / m_{max})

Three slabs S23, S24 and S25 compared to S1 control specimen showed in Table 4 to study effect top steel ratio/ μ_{max} on ultimate deflection, ultimate load and secant stiffness. It can be noted that a small increase in the ultimate load with big decrease in deflection led to large secant stiffness at increasing top steel ratio/ \square_{max} . the ultimate load and secant stiffness of slab S23 is less than of slab S1 by (12.5% and 11.63%) respectively, while S24 and S25 is larger than of slab S1 by (4.16% and 18.19%) and (12.5% and 47.27%) respectively. In addition to the ultimate deflection of slabS5 larger than of slab S1 by 11.65% but S6 and S7 is less than of slab S1 by11.87%, and 23.61% respectively.

V. COMPARISON OF THE NUMERICAL RESULTS AND THAT CALCULATED FROM EGYPTIAN CODE 203-2017 [1] AND ACI318-19 CODE [2]

The numerical results were compared with those calculated from the ECP 203-2017 [1] and ACI 318-19 [2] to verify the results as shown in Table 4.

V.I Comparison of the numerical results and that calculated from Egyptian code 203-2017 [1]

Table 5 illustrates the comparison between the numerical ultimate load and the ultimate load calculated from Egyptian code 203-2017 [1]. The mean of the ratio of the numerical ultimate load and that calculated using Egyptian code 203-2017 [1] is 119%, the standard deviation is 13% and coefficient of variation 11% for the twenty-four-slab used in the parametric study (S1 to S24), while these values for the last six slabs used in the parametric study (S25 to S32) are 106%, 15% and 14% respectively. This comparison reveals agreement between the numerical results and those calculated using the Egyptian code 203-2017 [1].

V.II Comparison of the numerical results and that calculated from ACI 318-19 code [2]

Good agreement between ACI 318-19 code [2] results and the nonlinear finite elements analysis was achieved. Table 4 shows the ratio between the numerical and ACI 318-19 code [2]; $P_{u Num} / P_{u ACI [2]}$. The mean of this ratio for the twenty-four-slab used in the parametric study (S1 to S24), the standard deviation and coefficient of variation are 111% 11% and 10% respectively, while these values for the last six slabs used in the parametric study (S25 to S32) are 116%, 15% and 13% respectively.

TABLE IV: COMPARISON OF P_u USING EGYPTIAN CODE 203-2017 [1] AND ACI 318-19 CODE [2] AND THE NUMERICaL REUSLTS.

Slab No.	NLFEA result	Codes results		NLFEA / Codes		Codes
	Ultimate load $P_{u Num.}$ (kN)	$P_{u Egy. [1]}$ (kN)	$P_{u ACI [2]}$ (kN)	$P_{u Num} / P_{u Egy. [1]}$	$P_{u Num} / P_{u A [2] CI}$	$P_{u Egy. [1]} / P_{u ACI [2]}$
1	1056	875.156	928.91	1.21	1.14	0.94
2	1188	941.6232	1017.57	1.26	1.17	0.92
3	1276	1034.622	1099.10	1.23	1.16	0.83
4	1364	1131.732	1174.99	1.20	1.16	0.75
Mean				1.23	1.16	0.83
S.D				0.03	0.006	0.08
C.O.V				0.02	0.005	0.10
5	968	875.156	928.91	1.07	1.01	0.94
6	1144	875.156	928.91	1.31	1.23	0.94
7	1188	875.156	928.91	1.36	1.28	0.94
Mean				1.25	1.17	0.94
S.D				0.15	0.14	0
C.O.V				0.12	0.12	0
8	1188	992.240	1053.19	1.20	1.13	0.94
9	1320	1113.293	1181.68	1.24	1.12	0.94
10	1452	1238.316	1314.38	1.17	1.10	0.94
Mean				1.21	1.11	0.94
S.D				0.03	0.15	0
C.O.V				0.03	0.01	0
11	968	875.156	928.91	1.11	1.04	0.94
12	1144	875.156	928.91	1.31	1.23	0.94
13	1232	875.156	928.91	1.41	1.33	0.94

Mean				1.27	1.2	0.94
S.D				0.16	0.15	0
C.O.V				0.12	0.12	0
14	968	875.156	928.91	1.11	1.04	0.94
15	880	875.156	928.91	1.01	0.95	0.94
16	792	875.156	928.91	0.91	0.86	0.94
Mean				1.01	0.95	0.94
S.D				0.1	0.09	0
C.O.V				0.99	0.095	0
17	792	696.553	739.34	1.13	1.07	0.94
18	1188	1051.949	1118.49	1.13	1.06	0.94
19	1364	1142.381	1308.06	1.19	1.04	0.87
Mean				1.15	1.06	0.92
S.D				0.03	0.015	0.04
C.O.V				0.03	0.014	0.044
20	968	875.156	928.91	1.11	1.04	0.94
21	1100	875.156	928.91	1.26	1.18	0.94
22	1232	875.156	928.91	1.40	1.32	0.94
Mean				1.26	1.18	0.94
S.D				0.14	0.14	0
C.O.V				0.11	0.12	0
23	924	875.156	928.91	1.05	0.99	0.94
24	1100	875.156	928.91	1.26	1.18	0.94
25	1188	875.156	928.91	1.36	1.28	0.94
Mean				1.22	1.15	0.94
S.D				0.16	0.15	0
C.O.V				0.13	0.13	0
Mean (total)				1.19	1.11	0.92
S.D (total)				0.13	0.11	0.04
C.O.V (total)				0.11	0.10	0.043

VI. CONCLUSIONS

The finite element (FE) analysis software program (ANSYS V. 19) was used to create the models and investigate the effects of some parameters on punching shear behavior of reinforced concrete flat slabs. Verification model was carried out to simulated a slab tested experimental by the first author. The numerical results compared with the experimental results. The results show that the numerical results matched with the experimental results and good agreement was archived. After that, some variables which included the effect of concrete compressive strength, reinforcing steel yield strength, slab thickness, shear studs diameter, shear studs spacing, shear studs distances from column face, main steel ratio/ μ_{max} , top steel ratio/ μ_{max} were studied. The numerical results were compared with the analytical results calculated from ECP 203-2017 [1] and ACI 318-19 [2] and the following are the main conclusions that can be drawn from the numerical and analytical results:

1. Finite element structural modeling simulated the experimental results up to good extent.
2. The higher the concrete compressive strength and slab thickness, the higher the ultimate load, secant stiffness and the lower the corresponding deflection.
3. The load deflection curves due to the of effect of the reinforcement yield strength are approximately the same at the beginning, while it varied according to the reinforcement ratio.
4. The higher the reinforcement yield strength, shear studs diameter, main steel, compression steel, the higher the ultimate load, secant stiffness and the lower the deflection at ultimate load.
5. The lower the shear studs spacing, the lower the ultimate load, secant stiffness and the higher the deflection at ultimate load.
6. The higher the shear studs distances from column face, the higher the ultimate load and secant stiffness while decreasing shear studs distances from column face, the lower the ultimate load, secant stiffness and the lower the deflection in both cases at ultimate load.

7. The mean and standard deviation demonstrate a good agreement between the numerical results and the analytical ones calculated from ECP 203-2017 [1] and ACI 318-19 [2].
8. The most results calculated from both ECP 203-2017 [1] and ACI [2] are less than that related to the numerical results this means that both Egyptian and ACI codes are conservative.
9. The results show that ACI 318-19 code [2] is more conservative than ECP 203-2017 [1].
10. ECP 203-2017 [1] and ACI [2] code provision should be revised to add the effect of reinforcement yield strength, shear studies (diameter, spacing) and flexural steel ratio (main and compression) on calculation punching shear capacity.

REFERENCES

- [1] Egyptian Code of Practice for Design and Construction of Reinforced Concrete Structures ECP-203, Housing and Building Research Center, Ministry of Building and Construction, Giza, Egypt, 2017, Chapter 6, pp. 113-122.
- [2] ACI Committee 318-19, Building Code Required for Reinforced Concrete, (ACI 318-19) and Commentary (ACI 318R-19), American Concrete Institute, Farmington Hills, Mich, 2019, Chapter 22, 4011-4020.
- [3] Jae, I.J. and Su, M. K., "Punching shear behavior of shear reinforced slab– column connection with varying flexural reinforcement", International Journal of Concrete Structures and Materials, ,2019.
- [4] Eid, F. M., "New methods for resisting punching shear stress in reinforced concrete flat slabs", Journal of Current Engineering and Technology, Vol.8, No.2, 2018.
- [5] Lips, S., Fernandez, M.R. and Muttoni, A., "Experimental investigation on punching strength and deformation capacity of shear-reinforced slabs", ACI Structural Journal, 109(1): 889–900, 2012.
- [6] Hamed, S. A., "Repair of R/C flat plates failing in punching by vertical studs", Alexandria Engineering Journal, 2015.
- [7] Malena, B. M., and Eugen, B., "Composite model for predicting the punching resistance of R-UHPFRC-RC composite slabs", Engineering Structures, 117, pp.603-616, 2016.
- [8] ANSYS Inc., Release 19.0, Documentation, Theory References, 2013.
- [9] Hanna, F.H.H., "External strengthening of reinforced concrete flat slabs to resist punching using different techniques", Ph.D. (under Discussion), Faculty of Engineering, Matarya, Helwan University, Civil Engineering Department, Structure, Egypt, 2021.